Acta Crystallographica Section C
Crystal Structure Communications
ISSN 0108-2701

Inter-ring and *endo* anomeric effects, and hydrogen-bonded supramolecular motifs in two 2,4,6,8-tetraazabicyclo-[3.3.0]octane derivatives

Zhenfeng Zhang,[a]* Jiange Wang,[b] Guisheng Zhang[a] and Jianpin Li[a]

[a]College of Chemistry and Environmental Science, Henan Normal University, Xinxiang 453007, People's Republic of China, and [b]College of Chemistry, Luoyang Normal University, Xinxiang 453007, People's Republic of China
Correspondence e-mail: zzf5188@sohu.com

Received 26 November 2008
Accepted 26 January 2009
Online 7 March 2009

In 2,4,6,8-tetrakis(4-chlorophenyl)-2,4,6,8-tetraazabicyclo-[3.3.0]octane, $C_{28}H_{22}Cl_4N_4$, the imidazolidine rings adopt envelope conformations, which are favoured by two equal *endo* anomeric effects. The molecule lies on a crystallographic twofold axis and molecules are linked into a three-dimensional framework *via* two C—H···Cl hydrogen bonds. In 2,4,6,8-tetrakis(4-methoxyphenyl)-2,4,6,8-tetraazabicyclo-[3.3.0]octane, $C_{32}H_{34}N_4O_4$, one of the methyl groups is disordered over two sets of sites and the same methyl group participates in an intermolecular C—H···O hydrogen bond, which in turn causes a considerable deviation from the preferred conformation. There are two unequal inter-ring anomeric effects in the N—C—N groups. Molecules are linked into corrugated sheets by one C—H···π hydrogen bond and two independent C—H···O hydrogen bonds involving methoxy groups.

Comment

Derivatives of tetrabicyclo[3.3.0]octane have been studied extensively. They have been synthesized either *via* hydride reduction of glycoluril derivatives or by condensation of amine with glyoxal and formaldehyde (Koppes *et al.*, 1987; Farnia & Kakanejadifard, 1992; Farnia *et al.*, 1993; Nielsen *et al.*, 1992). In addition, the anomeric effect in the N—C—N groups in 2,4,6,8-tetraphenyl-2,4,6,8-tetraazabicyclo[3.3.0]-octane, (I), has been investigated by X-ray analysis, showing that there are two interactions in the molecule: first, aromatic conjugation with ring N atoms, and second, two equal $n_N \rightarrow \sigma^*_{C-N}$ anomeric effects, best described as 'negative hyperconjugation' (Kakanejadifard & Farnia, 1997). In this article, we further investigate the effect of substituents at *para* positions of the phenyl rings on the anomeric effect in the N—C—N groups and on the molecular and supramolecular structures of two such compounds, namely 2,4,6,8-tetrakis(4-chlorophenyl)-2,4,6,8-tetraazabicyclo[3.3.0]octane, (II), and 2,4,6,8-tetrakis-(4-methoxyphenyl)-2,4,6,8-tetraazabicyclo[3.3.0]octane, (III) (Figs. 1 and 2, respectively).

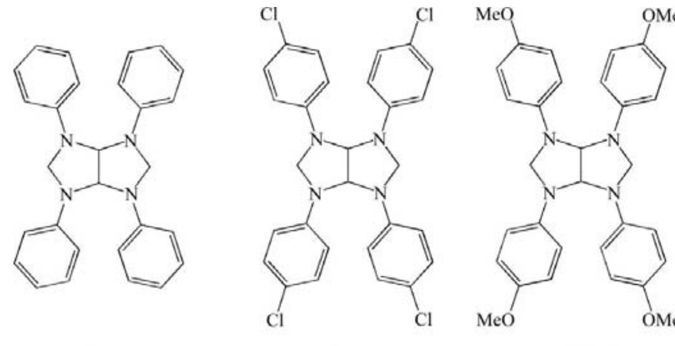

(I) (II) (III)

The molecule of (II) lies on a crystallographic twofold axis. The methine H atoms at the ring junction are in *cis* configurations. Each of the two fused imidazolidine rings adopts an envelope conformation; atoms N1 are the flap atoms, displaced by 0.545 (3) Å from the planes of the other four atoms. Interestingly, the two 4-chlorophenyl groups at the N1 atoms occupy axial positions and each of the N2—C2 bonds adopts an antiperiplanar orientation relative to the lone pair on N1. The orientation of N2—C2 bonds and 4-chlorophenyl groups at the N1 atoms are not incidentally caused by the crystal packing, but suggest the possible existence of anomeric effects in the N—C—N fragments. This can be further confirmed by some correlative geometric parameters (Table 1). The N2—C2 bonds are much longer than the N1—C2 bonds, which are slightly shorter than the accepted value for an N—Csp^3 bond (1.444–1.448 Å; Glidewell *et al.*, 2003; Feng *et al.*, 2004; Li *et al.*, 2005; Chandrasekhar *et al.*, 2007). The observed conformation, the remarkable lengthening of the N2—C2 bonds and the slightly shortening of the N1—C2 bonds all suggest that there are two equal *endo* anomeric effects in the N1—C2—N2 units that are best rationalized in terms of $n_{N1} \rightarrow \sigma^*_{C2-N2}$ stabilizing interactions. The inter-

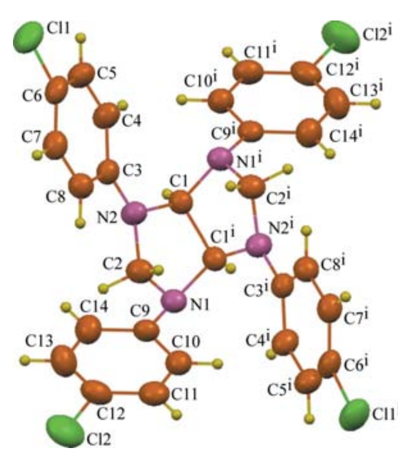

Figure 1
The molecular structure of (II), showing the atom-labelling scheme. Displacement ellipsoids are drawn at the 50% probability level. [Symmetry code: (i) $-x + 1, y, -z + \frac{1}{2}$.]

  doi:10.1107/S0108270109003242 *Acta Cryst.* (2009). C**65**, o146–o150

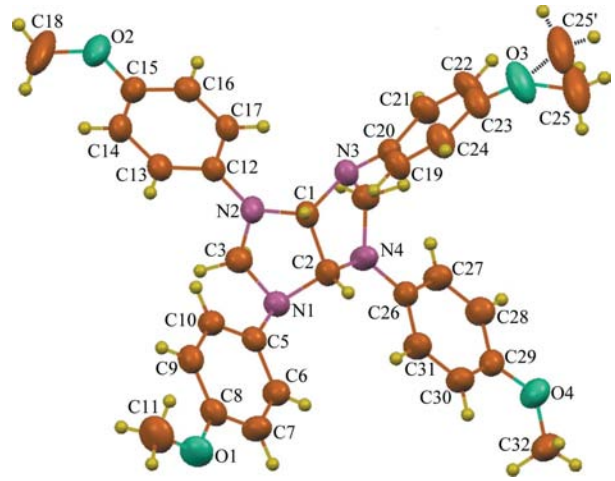

Figure 2
The molecular structure of (III), showing the atom-labelling scheme. Displacement ellipsoids are drawn at the 50% probability level.

actions require that the aromatic groups at atoms N1 occupy axial positions with respect to the corresponding imidazolidine rings and the N2—C2 bonds take antiperiplanar orientations relative to the N1 lone pairs.

As compared with (II), compound (III) presents some interesting structural features. As expected, the configurations for the methine H atoms at the ring junction are still of the *cis* form, and the two fused five-membered rings adopt envelope conformations; the flap atoms are N1 and N3, displaced by 0.465 (2) and 0.467 (3) Å, respectively, from the C1–C3/N2 and C1/C2/N4/C4 planes. The dihedral angle between the C1–C3/N2 and C1/C2/N4/C4 planes is 80.94 (2)° [the corresponding value in (II) is 83.07 (2)°]. This indicates that the two envelope planes take a nearly perpendicular orientation (Figs. 1 and 2). These features in conformation and configuration are similar to those found in (I) (Kakanejadifard & Farnia, 1997). The methoxy groups on atoms C8, C15 and C29 are effectively coplanar with their attached benzene rings, as shown by the corresponding torsion angles (Table 3). The situation is, however, different for the methoxy group on C22, where the methyl group is disordered over two sets of sites with refined occupancies of 0.653 (5) and 0.347 (5) (Fig. 2). The C25′ methyl group adopts a closely coplanar orientation to the C19–C24 ring though involved in a weak intermolecular C—H···O hydrogen bond, but C25 does not adopt the above similar preferred conformation, as shown by the C23—C22—O3—C25 torsion angles. The difference in conformation is mainly due to the fact that the methyl group (C25) takes part in a relatively strong intermolecular C—H···O hydrogen bond to a neighbouring methoxy group (Table 4 and Fig. 5), thus overcoming the van der Waals repulsion between the methyl group (C25) and the C19–C24 ring. Interestingly, the bond distances for (III) indicate that there are two progressive inter-ring anomeric effects in the N1—C2—N4 and N2—C1—N3 fragments, but not in the equivalent structural units (*i.e.* N1—C3—N2 and N3—C4—N4) as in (II), as evidenced by the shortening of the C1—N2 and C2—N4 bonds and the lengthening of the C1—N3 and C2—N1 bonds (Table 3). However, both of the unequal anomeric effects are best rationalized in terms of the 'negative hyperconjugation' of the *p*-electron pair on atom N2 or N4 with the adjacent anti-bonding orbital of C1—N3 or C2—N1.

In (II), there are no Cl···Cl or aromatic π–π stacking interactions; instead, molecules are linked into a complex three-dimensional framework by a combination of only two independent C—H···Cl hydrogen bonds (Table 2). Despite this complexity, the formation of the structure can be easily analysed in terms of three one-dimensional substructures. In the first substructure, atom C5 in the molecule at (x, y, z) acts as a hydrogen-bond donor to 4-chlorophenyl atom Cl2 in the molecule at (x, $1 - y$, $\frac{1}{2} + z$), so forming by inversion a centrosymmetric $R_2^2(24)$ (Bernstein *et al.*, 1995) ring centred at ($\frac{1}{2}$, $\frac{1}{2}$, $\frac{1}{2}$). Propagation by inversion of the hydrogen-bond motif then generates a $C_2^2(12)$ chain of rings running parallel to the [001] direction, with $R_2^2(24)$ rings centred at ($\frac{1}{2}$, $\frac{1}{2}$, $\frac{n}{2}$) (n = zero or integer) (Fig. 3). Similarly, $R_2^2(24)$ rings of the above type, as the backbone building units within the structure, are further linked by an independent C—H···Cl hydrogen bond (Table 2) to form the second substructure (Fig. 3). Phenyl atom C14 in the molecule at (x, y, z), part of the dimer centred at ($\frac{1}{2}$, $\frac{1}{2}$, 0), acts as a hydrogen-bond donor to atom Cl1 in the molecule at ($\frac{1}{2} - x$, $\frac{1}{2} + y$, $\frac{1}{2} - z$), which is part of the dimer centred at (0, 1, 0), thus forming by inversion an $R_4^4(16)$ ring centred at ($\frac{1}{4}$, $\frac{3}{4}$, 0). Further propagation by translation of this hydrogen-bond motif generates a $C_2^2(11)$ chain of rings along the [1$\bar{1}$0] direction, but this time with $R_4^4(16)$ rings centred at ($\frac{n}{2} - \frac{1}{4}$, $-\frac{n}{2} + \frac{5}{4}$, 0) ($n$ is zero or an integer). In the simplest way, the third substructure is constructed by way of a C—H···Cl hydrogen bond: atom C14 in the molecule at ($1 - x$, y, $\frac{1}{2} - z$) acts as a hydrogen-bond donor to atom Cl1 in the molecule at ($\frac{1}{2} + x$, $\frac{1}{2} + y$, z), so forming by translation a $C_2^2(11)$ chain running along [110] (Fig. 4). The combination of these three

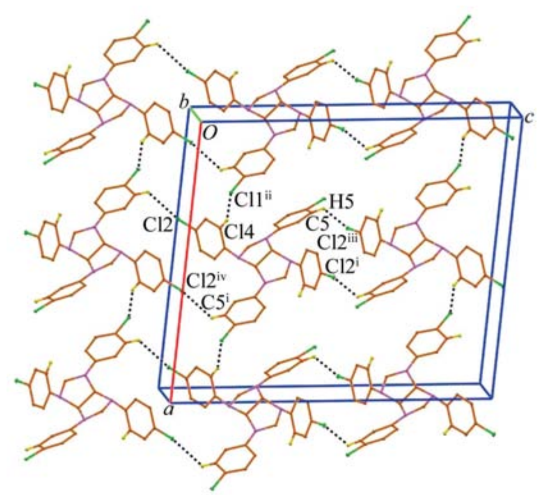

Figure 3
Part of the crystal structure of (II), showing the formation of a $C(24)$ chain of $R_2^2(24)$ rings parallel to the [001] direction and a $C_2^2(11)$ chain running along the [1$\bar{1}$0] direction. For the sake of clarity, H atoms not involved in the motif shown have been omitted. Intermolecular interactions are represented by dashed lines and selected atoms are labelled. [Symmetry codes: (i) $-x + 1, y, -z + \frac{1}{2}$; (ii) $-x + \frac{1}{2}, y + \frac{1}{2}, -z + \frac{1}{2}$; (iii) $x, -y + 1, z + \frac{1}{2}$; (iv) $-x + 1, -y + 1, -z$.]

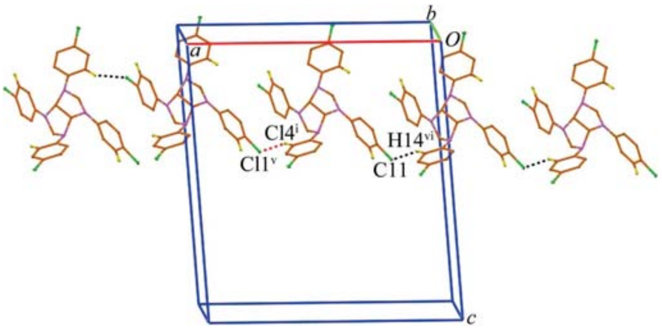

Figure 4
Part of the crystal structure of (II), showing the formation of a hydrogen-bonded chain along the [110] direction which is symmetry related to [1$\bar{1}$0]. For the sake of clarity, H atoms not involved in the motif shown have been omitted. Intermolecular interactions are represented by dashed lines and selected atoms are labelled. [Symmetry codes: (i) $-x + 1$, y, $-z + \frac{1}{2}$; (v) $x + \frac{1}{2}$, $y + \frac{1}{2}$, z; (vi) $-x + \frac{1}{2}$, $y - \frac{1}{2}$, $-z + \frac{1}{2}$.]

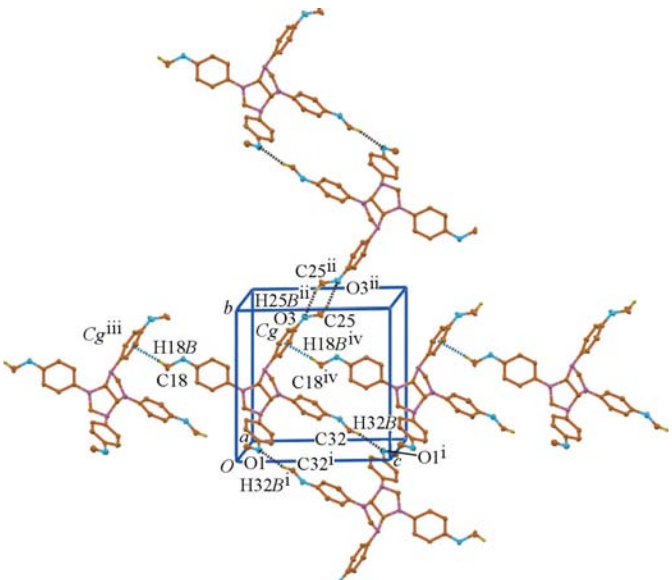

Figure 5
Part of the crystal structure of (III), showing the formation of a [001] chain and a chain of alternating $R_2^2(30)$ and $R_2^2(6)$ rings along [010]. Intermolecular interactions are represented by dashed lines and selected atoms are labelled. [Symmetry codes: (i) $-x + 1$, $-y$, $-z + 1$; (ii) $-x + 1$, $-y + 2$, $-z + 1$; (iii) x, y, $z - 1$; (iv) x, y, $z + 1$; *Cg* is the centroid of the C19–C24 ring.]

chain motifs links molecules of (II) into a three-dimensional framework.

The supramolecular structure of (III), by contrast, takes the form of a sheet by a combination of one C—H$\cdots\pi$ and two independent intermolecular C—H$\cdots$O hydrogen bonds involving methoxy groups (Table 4). However, the structure can be easily analysed in terms of two distinct low-dimensional substructures. For the sake of simplicity, we shall omit any consideration of the intermolecular interactions involving C25′, which are too weak to have any structural significance. In the first substructure, methoxy atom C32 in the molecule at (x, y, z) acts as a hydrogen-bond donor, *via* atom H32*B*, to atom O1 in the molecule at ($1 - x$, $-y$, $1 - z$), so generating by inversion an $R_2^2(30)$ ring centred at ($\frac{1}{2}$, 0, $\frac{1}{2}$) (Fig. 5), and methoxy atom C25 in the molecule at (x, y, z) acts as a hydrogen-bond donor, *via* atom H25*B*, to methoxy atom O3 in the molecule at ($1 - x$, $2 - y$, $1 - z$), thus generating by inversion a second centrosymmetric ring, this time of $R_2^2(6)$ type and centred at ($\frac{1}{2}$, 1, $\frac{1}{2}$) (Fig. 5). The combination of these two motifs generates a chain of edge-fused rings running parallel to the [010] direction, with R_2^2 (30) rings centred at ($\frac{1}{2}$, $2n$, $\frac{1}{2}$) (n = zero or integer) alternating with $R_2^2(6)$ rings centred at ($\frac{1}{2}$, $2n + 1$, $\frac{1}{2}$) (n = zero or integer) (Fig. 5). In the second one-dimensional substructure, methyl atom C18 in the molecule at (x, y, z) acts as a hydrogen-bond donor, *via* atom H18*B*, to the C19–C24 ring in the molecule at (x, y, $-1 + z$), so generating by translation a chain running along [001]. The combination of these two chain motifs is sufficient to link all the molecules into a corrugated two-dimensional sheet parallel to (011). Two such sheets pass through each unit cell in the same domain $0 < x < 1$, but there are no direction-specific interactions between the two sheets.

Accordingly, the anomeric effect and the supramolecular structures in (II) and (III) described here show some marked variations consequent upon changes of the *para*-position atoms of the aryl ring. Whereas compound (II), containing 4-chloro substituents and therefore possessing low lone-pair electronic density on the N atoms compared with (III), exhibits *endo* anomeric effects described as $n_N \rightarrow \sigma^*_{C-N}$ and aggregates into a three-dimensional structure by C—H$\cdots$Cl hydrogen bonds, compound (III), containing 4-methoxy substituents and possessing high electronic density on the N atoms, exhibits inter-ring anomeric effects best described as the 'negative hyperconjugation' of the *p*-electron pair on an N atom with the adjacent antibonding C—N orbital, and forms a sheet structure *via* C—H$\cdots$O hydrogen bonds involving methyl groups.

Experimental

To a mixture of aqueous formaldehyde (0.2 mol) and aqueous glyoxal (0.1 mol) in ethanol (95%, 100 ml) were added 4-chloroaniline (or 4-methoxyaniline) (0.4 mol) and a catalytic amount of acetic acid (1 ml). The resulted mixture was refluxed with stirring for *ca* 10 min, then allowed to stand for 1 h at room temperature to precipitate the product completely. The precipitate was filtered off, washed with ethanol (95%) and dried to give the crystalline product (II) [or (III)]. Crystals of (II) were obtained by recrystallization from acetonitrile. ^{1}H NMR (DMSO, 400 MHz): δ 7.19–6.91 (*dd*, 16H), 6.38 (*s*, 2H), 4.80–4.58 (*AB$_q$*, J = 7.8 Hz, 4H). Crystals of (III) were obtained by recrystallization from ethyl acetate. ^{1}H NMR (DMSO, 400 MHz): δ 6.86–6.74 (*dd*, 16H), 6.02 (*s*, 2H), 4.60–4.53 (*AB$_q$*, J = 7.2 Hz, 4H), 3.64 (*s*, 12H).

Compound (II)

Crystal data

$C_{28}H_{22}Cl_4N_4$	V = 2481 (3) Å^3
M_r = 556.30	Z = 4
Monoclinic, $C2/c$	Mo $K\alpha$ radiation
a = 19.368 (15) Å	μ = 0.50 mm^{-1}
b = 5.880 (4) Å	T = 294 (2) K
c = 21.894 (16) Å	0.40 × 0.19 × 0.15 mm
β = 95.602 (9)°	

Table 1
Selected geometric parameters (Å, °) for (II).

N1—C9	1.433 (2)	N2—C3	1.396 (2)
N1—C2	1.443 (2)	N2—C2	1.471 (2)
C9—N1—C2	118.79 (15)	C3—N2—C2	119.50 (14)
C9—N1—C1^{i}	114.23 (14)	C1—N2—C2	109.29 (14)
C2—N1—C1^{i}	103.49 (14)		

Symmetry code: (i) $-x+1, y, -z+\frac{1}{2}$.

Table 2
Hydrogen-bond geometry (Å, °) for (II).

D—H···A	D—H	H···A	D···A	D—H···A
C14—H14···Cl1^{ii}	0.93	2.80	3.668 (3)	156
C5—H5···Cl2^{iii}	0.93	2.90	3.541 (3)	127

Symmetry codes: (ii) $-x+\frac{1}{2}, y+\frac{1}{2}, -z+\frac{1}{2}$; (iii) $x, -y+1, z+\frac{1}{2}$.

Data collection

Bruker SMART CCD area-detector diffractometer
Absorption correction: multi-scan (*SADABS*; Sheldrick, 2003)
T_{min} = 0.813, T_{max} = 0.930
7355 measured reflections
2271 independent reflections
1821 reflections with $I > 2\sigma(I)$
R_{int} = 0.022

Refinement

$R[F^2 > 2\sigma(F^2)]$ = 0.033
$wR(F^2)$ = 0.082
S = 1.03
2271 reflections
163 parameters
H-atom parameters constrained
$\Delta\rho_{max}$ = 0.19 e Å^{-3}
$\Delta\rho_{min}$ = −0.21 e Å^{-3}

Compound (III)

Crystal data

$C_{32}H_{34}N_4O_4$
M_r = 538.63
Triclinic, $P\overline{1}$
a = 9.889 (4) Å
b = 11.996 (5) Å
c = 12.312 (5) Å
α = 89.495 (5)°
β = 74.381 (5)°
γ = 82.332 (5)°
V = 1393.6 (11) Å^3
Z = 2
Mo $K\alpha$ radiation
μ = 0.09 mm^{-1}
T = 291 (2) K
0.48 × 0.41 × 0.25 mm

Data collection

Bruker SMART CCD area-detector diffractometer
Absorption correction: multi-scan (*SADABS*; Sheldrick, 2003)
T_{min} = 0.828, T_{max} = 0.979
10373 measured reflections
5134 independent reflections
4059 reflections with $I > 2\sigma(I)$
R_{int} = 0.019

Refinement

$R[F^2 > 2\sigma(F^2)]$ = 0.041
$wR(F^2)$ = 0.111
S = 1.02
5134 reflections
370 parameters
34 restraints
H-atom parameters constrained
$\Delta\rho_{max}$ = 0.17 e Å^{-3}
$\Delta\rho_{min}$ = −0.22 e Å^{-3}

All H atoms were placed in idealized positions and allowed to ride on their respective parent atom, with C—H distances of 0.93 (aromatic), 0.96 (CH_3), 0.97 (CH_2) or 0.98 Å (CH) and U_{iso}(H) values of 1.2 times U_{eq}(C) (1.5 for methyl H atoms). The methyl groups on atoms O2 and O3 in (III) were found to be disordered. Atom C25 was modelled over two sets of positions, with a refined major occupancy of 65.3 (5)%. Geometric displacement-parameter restraints were applied to the disordered methyl group. No disorder model was applied for C18 because the ellipsoid was slightly less extreme.

Table 3
Selected geometric parameters (Å, °) for (III).

C25—O3	1.451 (3)	N2—C3	1.461 (2)
N1—C5	1.447 (2)	N3—C19	1.424 (2)
N1—C2	1.482 (2)	N3—C1	1.464 (2)
N2—C12	1.392 (2)	N4—C2	1.443 (2)
N2—C1	1.448 (2)		
C5—N1—C3	114.97 (12)	C1—N3—C4	104.20 (11)
C5—N1—C2	113.05 (11)	C26—N4—C2	123.42 (12)
C12—N2—C1	122.15 (12)	C26—N4—C4	122.16 (12)
C12—N2—C3	124.92 (12)	C2—N4—C4	111.30 (12)
C1—N2—C3	111.00 (12)	N2—C1—N3	111.65 (12)
C19—N3—C1	119.72 (11)	N4—C2—N1	113.25 (12)
C19—N3—C4	115.99 (11)		

Table 4
Hydrogen-bond geometry (Å, °) for (III).

Cg is the centroid of the C19–C24 ring.

D—H···A	D—H	H···A	D···A	D—H···A
C32—H32*B*···O1^{i}	0.96	2.59	3.169 (2)	119
C25—H25*B*···O3^{ii}	0.96	2.57	3.499 (4)	164
C18—H18*B*···*Cg*^{iii}	0.96	2.60	3.54 (3)	167

Symmetry codes: (i) $-x+1, -y, -z+1$; (ii) $-x+1, -y+2, -z+1$; (iii) $x, y, z-1$.

For both compounds, data collection: *SMART* (Bruker, 1997); cell refinement: *SAINT* (Bruker, 1997); data reduction: *SAINT*; program(s) used to solve structure: *SHELXS97* (Sheldrick, 2008); program(s) used to refine structure: *SHELXL97* (Sheldrick, 2008); molecular graphics: *SHELXTL* (Sheldrick, 2008); software used to prepare material for publication: *SHELXTL*.

Financial support from Henan Normal University, the Natural Science Foundation of Henan Province (grant No. 0611021700) and the 'Innovation Scientists and Technicians Troop Construction Projects of Henan Province' (grant No. 2008IRTSTHN002) is gratefully acknowledged. The authors are grateful to the Physiochemical Analysis Measurement College of Chemistry, Luoyang Normal University, for providing the X-ray analysis.

Supplementary data for this paper are available from the IUCr electronic archives (Reference: FN3008). Services for accessing these data are described at the back of the journal.

References

Bernstein, J., Davis, R. E., Shimoni, L. & Chang, N.-L. (1995). *Angew. Chem. Int. Ed. Engl.* **34**, 1555–1573.
Bruker (1997). *SMART* and *SAINT*. Bruker AXS Inc., Madison, Wisconsin, USA.
Chandrasekhar, S., Chopra, D., Gopalaiah, K. & Guru Row, T. N. (2007). *J. Mol. Struct.* **837**, 118–131.
Farnia, S. M. F. & Kakanejadifard, A. (1992). *Iran. J. Chem. Chem. Eng.* **11**, 39–41.
Farnia, S. M. F., Kakanejadifard, A., Karimi, S. & Todaro, L. J. (1993). *Iran. J. Chem. Chem. Eng.* **12**, 57–60.

Feng, C.-G., Fang, H. & Huang, P.-Q. (2004). *Acta Cryst.* E**60**, o1075–o1077.
Glidewell, C., Low, J. N., Skakle, J. M. S. & Wardell, J. L. (2003). *Acta Cryst.* C**59**, o207–o209.
Kakanejadifard, A. & Farnia, M. F. (1997). *Tetrahedron*, **53**, 2551–2556.
Koppes, W. M., Chaykovsky, M., Adolph, H. G., Gilardi, R. D. & George, C. F. (1987). *J. Org. Chem.* **52**, 1113–1119.
Li, Y.-T., Zhou, B.-H., Yin, G.-D. & Wu, A.-X. (2005). *Acta Cryst.* E**61**, o3368–o3370.
Nielsen, A. T., Nissan, R. A., Chafin, A. P., Gilardi, R. D. & George, C. F. (1992). *J. Org. Chem.* **57**, 6756–6759.
Sheldrick, G. M. (2003). *SADABS*. University of Göttingen, Germany.
Sheldrick, G. M. (2008). *Acta Cryst.* A**64**, 112–122.